

SUPERNOVAE EXPLOSIONS INDUCED BY PAIR-PRODUCTION INSTABILITY*

GARY S. FRALEY**

California Institute of Technology, Pasadena, Calif., U.S.A.

(Received 29 March, 1968)

Abstract. Stars with a core mass greater than about $30 M_{\odot}$ become dynamically unstable due to electron-positron pair production when their central temperature reaches $1.5\text{--}2.0 \times 10^9 \text{ K}$. The collapse and subsequent explosion of stars with core masses of 45, 52, and $60 M_{\odot}$ is calculated. The range of the final velocity of expansion (3400–8500 km/sec) and of the mass ejected ($1\text{--}40 M_{\odot}$) is comparable to that observed for type II supernovae. A dynamical model of convection is derived and included in the calculations. It was found that the effect of the convection on the explosions is probably not important.

1. Introduction

In investigations of the origins of supernovae, the usual cause of stellar collapse considered has been the decomposition of iron at temperatures around $5\text{--}6 \times 10^9 \text{ K}$. Calculations of the collapse have been carried out by COLGATE and WHITE (1966), and by ARNETT (1967). Recently, RAKAVY and SHAVIV (1966) have found another cause of dynamic instability; stars of more than about $30 M_{\odot}$ become unstable due to the formation of electron-positron pairs. The absorption of energy to create the rest mass of the pairs lowers the value of $\gamma = d \log P / d \log \rho$, below $\frac{4}{3}$ at low densities (see Figure 1). The number of pairs decrease exponentially at low temperatures; at high temperatures, the energy absorbed in creating the rest mass becomes less significant. The result is that the boundary of the 'unstable area' (where γ is less than $\frac{4}{3}$) reaches a maximum density of about $7 \times 10^5 \text{ gm/cm}^3$ at a temperature of $2.8 \times 10^9 \text{ K}$. When a sufficient amount of the star has entered this area, it becomes dynamically unstable and begins to collapse. This occurs only for massive stars, since lower mass stars evolve along density-temperature lines that always keep them above the unstable area.

The collapse due to pair production is quite mild compared to that due to iron decomposition. After a compression of less than 10, a sufficient portion of the star will have passed out of the unstable area on its high temperature boundary. The resultant stiffening (i.e., the pressure increases faster than the gravitational forces) reverses the collapse. The temperatures reached near the center in a typical case produce oxygen burning at an explosive rate. Providing enough oxygen is burned, the energy released will disrupt all or part of the star, and eject the material with high velocities. The energy released in oxygen burning is about equal to a kinetic energy of

* Work supported in part by the U.S. National Aeronautics and Space Administration under Grant NsG-426.

** Present address: Los Alamos Scientific Laboratory, Los Alamos, N.M., U.S.A.

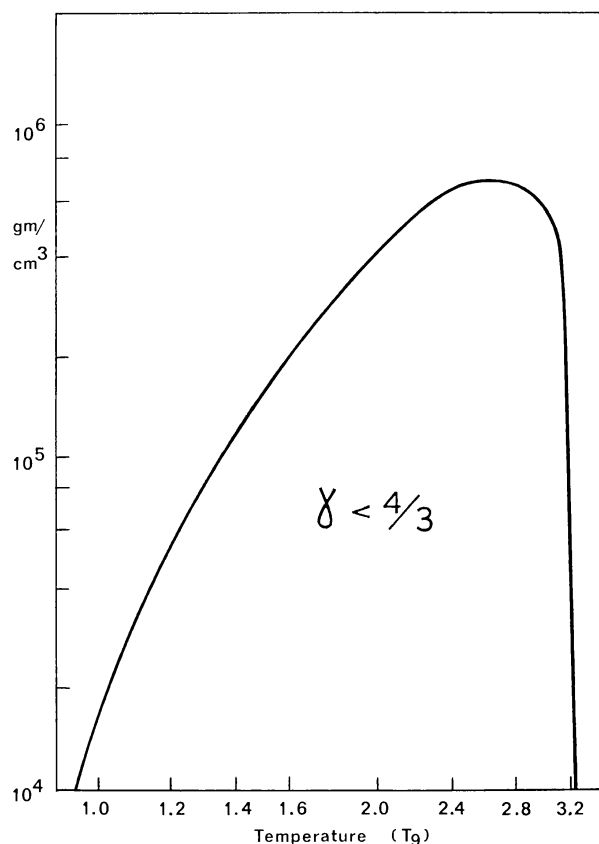


Fig. 1. The area in which γ becomes less than $\frac{4}{3}$ due to electron-positron pair production.

10000 km/sec. This then should be something of an upper limit for the (average) velocity of expansion.

More massive stars with higher entropies become unstable at lower temperatures. During the collapse they acquire a greater inward momentum, and reach a higher temperature at the reversal of collapse. There is a greater energy release from the oxygen burning, and so the explosion following the collapse is of greater intensity. For sufficiently massive stars (e.g., greater than $100 M_{\odot}$), the collapse may proceed until the center reaches a temperature at which the heavier elements (silicon, iron) begin to decompose. In that case γ remains less than $\frac{4}{3}$ at the center, and the collapse may never be reversed. This paper investigates the collapse and explosion of stars of masses (45, 52, and $60 M_{\odot}$) intermediate between this possible upper limit and the lower limit of about $30 M_{\odot}$.

Two principal problems are the numerical techniques used in calculating the hydrodynamics, and the effects of convective instability. The usual method of dealing with the hydrodynamics is the explicit one which is stable only if the time step is less than the Courant limit (the time it takes sound to cross a mass zone). For comparatively slow evolution, conditions change only slightly during a time step so restricted it is then preferable to take larger steps. This may be done by an implicit hydrodynamic;

scheme which is used here. The way in which quantities, including the force, are averaged over the time step is allowed to vary. One of the special cases reduces essentially to hydrostatic equilibrium; this is used when appropriate (see Appendix).

For evolution on a dynamical time-scale, convective instability does not produce the zero entropy gradient and perfect mixing which is found for slower evolution. A simple model of the convection, which gives in a rough fashion the results of the instability, and which is easily incorporated into the scheme of the numerical calculation (see Appendix), is derived from the equations of motion. Besides the equations of motion, we then also have the equations for the time derivatives of the kinetic energy of the convective turbulence, and of the convective energy flux. This method, while giving the interaction of the turbulence with the material, does not, of course, give the self-interaction of the turbulence, which is responsible, e.g., for the decay of the turbulent energy. This must be estimated by other means.

2. Convection

A. INTRODUCTION

The general method used here for the derivation of the convective model is that used by COWLING (1936). The velocity U is divided into the mean velocity V and the convective velocity W . The latter is defined so that it does not, on the average, effect any net mass transport or possess momentum. For spherical symmetry, the averaging is done by integrating over a spherical shell.

$$\langle \rho U_i \rangle = \langle \rho V_i \rangle + \langle \rho W_i \rangle = \langle \rho \rangle V_i, \quad i = 1, 2, 3,$$

where V_i remains constant over the area of averaging. The kinetic energy may be divided into the energy of the mean motion and that of the convective turbulence, the latter being, in a sense, a form of internal energy.

$$\langle \frac{1}{2} \rho U_i U_i \rangle = \frac{1}{2} \langle \rho \rangle V_i V_i + \frac{1}{2} \langle \rho W_i W_i \rangle.$$

A pair of the same indices indicates a summation.

The equations of motion are averaged in the same way. The equations for the conservation of mass, energy, and momentum are:

$$\frac{\partial \rho}{\partial t} + \nabla_i (\rho U_i) = 0, \quad (1)$$

$$\frac{\partial (\rho E)}{\partial t} + \nabla_i (\rho E U_i) + P \nabla_i U_i = \rho \varepsilon - \nabla_i F_i - P_{ij} \nabla_j U_i, \quad (2)$$

and

$$\frac{\partial (\rho U_i)}{\partial t} + \nabla_j (\rho U_j U_i) = \rho G_i - \nabla_i P - \nabla_j P_{ij}, \quad (3)$$

where P_{ij} is the viscosity stress tensor, G_i is the external force, and F_i is the energy flux.

When averaged, the equations are

$$\frac{D\langle\rho\rangle}{Dt} + \langle\rho\rangle \nabla_i V_i = 0, \quad (4)$$

$$\begin{aligned} \langle\rho\rangle \frac{D}{Dt} (\langle\rho E\rangle/\langle\rho\rangle) + \langle\rho\rangle \langle P\rangle \frac{D\langle v\rangle}{Dt} = & -\langle\nabla_i(\rho E W_i)\rangle - \langle P \nabla_i W_i\rangle \\ & + \langle\rho \varepsilon\rangle - \langle\nabla_i F_i\rangle - \langle P_{ij} \nabla_j U_i\rangle, \end{aligned} \quad (5)$$

and

$$\langle\rho\rangle \frac{DV_i}{Dt} = \langle\rho G_i\rangle - \langle\nabla_i P\rangle - \langle\nabla_j(\rho W_i W_j)\rangle, \quad (6)$$

where $D/Dt = \partial/\partial t + V_i \nabla_i$, i.e., a derivative which follows the mean motion of the material. The averaged momentum equation differs from the original by the presence of the Reynolds stresses. The basic difference in the energy equation is the convective energy flux, $\langle\rho E W_i\rangle$. The second term on the right-hand side generally acts to reinforce the convective flux. The effect of viscosity on the mass motion has been neglected; the viscosity term in the energy equation then represents heat formed by the decay of the turbulent kinetic energy.

For spherical symmetry, the derivative of the radial velocity is

$$\langle\rho\rangle \frac{DV_r}{Dt} = \langle\rho G_r\rangle - \frac{\partial\langle P\rangle}{\partial r} - \left[\frac{\partial}{\partial r} (r^2 \langle\rho W_r^2\rangle) - r \langle\rho W_\theta^2\rangle - r \langle\rho W_\phi^2\rangle \right] \frac{1}{r^2}. \quad (7)$$

For simplicity, the distribution of the kinetic energy of the turbulence is assumed to be isotropic, i.e.,

$$\langle\rho W_r^2\rangle = \langle\rho W_\theta^2\rangle = \langle\rho W_\phi^2\rangle,$$

and Equation (7) becomes

$$\langle\rho\rangle \frac{DV_r}{Dt} = \langle\rho G_r\rangle - \frac{\partial}{\partial r} (\langle P\rangle + \langle\rho W_r^2\rangle). \quad (8)$$

Besides the usual equations of motion there are required the equations for the turbulent kinetic energy and the convective energy flux. Equation (3) is contracted with U_i to give the rate of change of the total kinetic energy

$$\begin{aligned} \frac{D}{Dt} \langle \tfrac{1}{2} \rho U_i U_i \rangle + \langle \tfrac{1}{2} \rho U_i U_i \rangle \nabla_j V_j + \langle \nabla_j (W_j \tfrac{1}{2} \rho U_i U_i) \rangle \\ = \langle U_i \rho G_i \rangle - \langle U_i \nabla_i P \rangle - \langle U_i \nabla_j P_{ij} \rangle. \end{aligned} \quad (9)$$

The derivative of the energy of the mean motion (obtained by contracting Equation (6) with V_i) is subtracted; this leaves that of the turbulent energy.

$$\begin{aligned} \langle\rho\rangle \frac{D}{Dt} (\langle \tfrac{1}{2} \rho W_i W_i \rangle / \langle\rho\rangle) = & -\langle W_i \nabla_i P \rangle - \langle W_i \nabla_j P_{ij} \rangle \\ & - \langle \nabla_j (W_j \tfrac{1}{2} \rho W_i W_i) \rangle - \langle \rho W_i W_j \nabla_j V_i \rangle. \end{aligned} \quad (10)$$

B. TREATMENT OF THE TURBULENT ENERGY AND ENERGY FLUX

It will be assumed that the density fluctuations over an area of averaging are small. Then the energy flux is proportional to the averaged convective velocity.

$$\begin{aligned} L_i \equiv \langle \rho E W_i \rangle &\approx \left\langle \left[\langle E \rangle + \left\langle \frac{dE}{d\rho} \right\rangle (\rho - \langle \rho \rangle) \right] \rho W_i \right\rangle \\ &= \left\langle \frac{dE}{d\rho} \right\rangle \langle \rho^2 W_i \rangle \approx - \left\langle \frac{dE}{d\rho} \right\rangle \langle \rho \rangle^2 \langle W_i \rangle. \end{aligned} \quad (11)$$

Usually the pressure fluctuations (those correlated with the convective velocity) should be small compared to the density fluctuations. In that case,

$$\left\langle \frac{dE}{d\rho} \right\rangle \approx \left\langle \left(\frac{\partial E}{\partial \rho} \right)_P \right\rangle.$$

The first term on the right of Equation (10) is the basic driving force. Under hydrostatic equilibrium its value is $-\langle \rho \rangle g \langle W \rangle$. Since the term $g \langle \rho W \rangle$ may be added to it, it is also equal to $g \langle (\Delta \rho) W \rangle$, showing that the turbulence is created by buoyancy forces. Whether or not the buoyancy effect acts to increase or decrease the turbulent energy depends on how the density fluctuations are correlated with the convective velocity, and this, of course, ultimately depends on whether or not the area is convectively stable or not. The effect is proportional to the energy flux (neglecting the pressure fluctuations).

The second term, the viscous dissipation of the turbulence, is approximated by $\langle \rho \rangle^{\frac{1}{3}} \langle W_i W_i \rangle^{1.5} / l$; l is roughly the length of those eddies which have the maximum energy (BATCHELOR, 1953). This should be reasonably valid providing the eddies have a large Reynolds number. These large eddies do not lose their energy directly into heat, but rather transfer it ultimately to small eddies, roughly in equilibrium, with Reynolds number of order one, which pass the energy on into heat. The factor l is more or less the equivalent of a mixing length. Since the larger the eddy the slower it decays, l should be about the size of the (smallest) characteristic length of the system, as it is expected that the largest eddies formed are of this size. For convection in stellar atmospheres, the mixing length is often taken equal to a scale height. However, the eddy size should not usually be larger than the radius, which near the center is less than a scale height. The procedure adopted was to make l proportional to the minimum of the pressure scale height, the radius, and the length of the convective zone itself. The constant of proportionality could be changed to determine what effect this might have on the evolution of the system.

The third term is the diffusion of the convective energy. It tends to spread out the turbulence evenly; it also introduces it to regions previously stable. It disappears when integrated over the entire turbulent zone. In estimating its magnitude, the derivative can be replaced by $1/l$, since the energy should not change substantially in a smaller distance. Since to a first approximation it cancels out, it is generally small compared to the dissipation. For simplicity, it is neglected here. It is responsible for spreading

the turbulence beyond the convectively unstable area; however, here it will be assumed that the turbulence effectively stops at the edge of the convectively unstable zone (except for decaying turbulence in a previously unstable region). Another effect is to transport energy. As long as the speed of convection is small compared to the speed of sound, this is considerably smaller than the flux of internal energy ($L \approx \langle |\Delta\rho| \rangle \langle |W| \rangle \langle E \rangle$).

For isotropic turbulence, the last term is

$$- \langle \rho \rangle \langle \rho W_r^2 \rangle \frac{D \langle v \rangle}{Dt}.$$

For spherical symmetry, Equation (10) is

$$\frac{D}{Dt} (\langle 1.5 \rho W_r^2 \rangle / \langle \rho \rangle) = \frac{L_r \frac{\partial \langle P \rangle}{\partial r}}{\langle \rho \rangle^3 \left\langle \frac{dE}{d\rho} \right\rangle} - \frac{\langle |W_r|^3 \rangle}{l} - \langle \rho W_r^2 \rangle \frac{D \langle v \rangle}{Dt}. \quad (12)$$

The derivative of the energy flux is

$$\begin{aligned} \frac{D}{Dt} \langle \rho E W_i \rangle &= \left\langle \rho E \frac{D}{Dt} (U_i - V_i) \right\rangle + \left\langle W_i \frac{D}{Dt} (\rho E) \right\rangle = \langle \rho E W_j \nabla_j W_i \rangle_1 \\ &\quad - \langle \rho E W_j \nabla_j V_i \rangle_2 + \frac{\langle \rho E \rangle}{\langle \rho \rangle} \langle \nabla_j (\rho W_i W_j) \rangle_3 \\ &\quad - \left(\langle E \nabla_i P \rangle - \frac{\langle \rho E \rangle}{\langle \rho \rangle} \langle \nabla_i P \rangle \right)_4 - \left(\langle E \nabla_j P_{ij} \rangle - \frac{\langle \rho E \rangle}{\langle \rho \rangle} \langle \nabla_j P_{ij} \rangle \right)_5 \\ &\quad - \langle W_i \rho E \nabla_j V_j \rangle_6 - \langle W_i E \nabla_j (\rho W_j) \rangle_7 - \langle W_i W_j \rho \nabla_j E \rangle_8 \\ &\quad + \left\langle \frac{W_i P}{\rho} \frac{D \rho}{Dt} \right\rangle_9 + \left\langle \frac{P}{\rho} W_i W_j \nabla_j \rho \right\rangle_{10} + \langle \rho \varepsilon W_i \rangle_{11} \\ &\quad - \langle W_i \nabla_j F_j \rangle_{12} - \langle W_i P_{kj} \nabla_j U_k \rangle_{13}. \end{aligned} \quad (13)$$

The approximate values for the terms on the right-hand side for the radial component of the flux are given below. Terms 1, 3, and 7 give

$$- \left[\langle E \nabla_j (W_i W_j \rho) \rangle - \frac{\langle \rho E \rangle}{\langle \rho \rangle} \langle \nabla_j (W_i W_j \rho) \rangle \right].$$

This reflects the fact that the Reynolds stresses tend to have a greater effect on the lighter, usually more energetic, elements. Similarly, term 4,

$$- \left[\langle E \nabla_i P \rangle - \frac{\langle \rho E \rangle}{\langle \rho \rangle} \langle \nabla_i P \rangle \right],$$

indicates the greater acceleration given the lighter elements by the pressure gradient. The effect is usually to increase the energy flux. Both terms are of the order of

$$\langle E \rangle \frac{\langle \rho E \rangle}{\langle \rho \rangle} \approx - \left\langle \frac{dE}{d\rho} \right\rangle \frac{\langle (\Delta\rho)^2 \rangle}{\langle \rho \rangle}.$$

As the square of the density fluctuations is supposed to be small, these will be neglected. Terms 2 and 6 are

$$-\langle \rho E W_r \rangle \frac{2V_r}{r} - \langle \rho E W_r \rangle 2 \frac{\partial V_r}{\partial r}.$$

Terms 8 and 10 give

$$-\langle \rho W_r^2 \rangle \left[\frac{\partial \langle E \rangle}{\partial r} + \langle P \rangle \frac{\partial \langle v \rangle}{\partial r} \right].$$

This is the entropy gradient (except for the effects of composition gradients). It is the basic driving force that with the buoyancy effect in Equation (10) creates the turbulence and energy flow. Term 9 is usually small and is neglected. Term 11 is caused by the difference in the rate of energy generation between the hot and cold elements. As nuclear reactions are strongly temperature dependent, it may be significant in some cases. Below a certain value of the speed of convection, the energy gained is greater than that loss by the mixing of hot and cool elements. Its value is

$$\langle \rho E W_r \rangle \left\langle \frac{d\varepsilon}{dE} \right\rangle.$$

Term 12 is dissipation by radiation from hot to cool elements. As these are separated by a distance of about l , this is roughly

$$\langle |W_r| \rangle \left\langle \frac{4acT^3}{3\kappa\rho} \frac{dT}{d\rho} \right\rangle \frac{2}{l^2} |\delta\rho|,$$

where $\delta\rho$ is the difference in density between the hot and cold elements. It is also approximately

$$-\frac{4}{l^2} \left\langle \frac{4acT^3}{3\kappa\rho} \frac{dT}{d\rho} \right\rangle \frac{L_r}{\langle \rho \rangle \left\langle \frac{dE}{d\rho} \right\rangle}.$$

The viscous effects (terms 5 and 13) should not have an important direct effect on the large eddies responsible for the energy transport. The same rate of turbulent dissipation used in Equation (12) will be used here. For the radial flux, Equation (13) is then

$$\begin{aligned} \frac{1}{r^2} \frac{D}{Dt} (r^2 L_r) = & -\langle \rho W_r^2 \rangle \left(\frac{\partial \langle E \rangle}{\partial r} + \langle P \rangle \frac{\partial \langle v \rangle}{\partial r} \right) \\ & + L_r \left[\left\langle \frac{d\varepsilon}{dE} \right\rangle - 2 \frac{\partial V_r}{\partial r} - \frac{\langle |W_r| \rangle}{l} - \frac{4}{l^2} \frac{\left\langle \frac{4acT^3}{3\kappa\rho} \frac{dT}{d\rho} \right\rangle}{\langle \rho \rangle \left\langle \frac{dE}{d\rho} \right\rangle} \right]. \quad (14) \end{aligned}$$

When Equations (12) and (5) are combined, the derivative for the total 'internal'

energy becomes

$$\begin{aligned} \langle \rho \rangle \left[\frac{D}{Dt} (\langle \rho E \rangle / \langle \rho \rangle + \langle 1.5 \rho W_r^2 \rangle / \langle \rho \rangle) + (\langle P \rangle + \langle \rho W_r^2 \rangle) \frac{D \langle v \rangle}{Dt} \right] \\ = \langle \rho \epsilon \rangle - \frac{1}{r^2} \frac{\partial}{\partial r} [r^2 \langle W_r (\rho E + P) \rangle + r^2 \langle F_r \rangle]. \end{aligned} \quad (15)$$

The effective energy flux is thus gotten by replacing the energy with the enthalpy. We now show that the equations developed are consistent with and predict the condition for convective instability. When the terms that are usually not important initially are eliminated, Equations (12) and (14) are

$$\frac{DL_r}{Dt} = - \langle \rho W_r^2 \rangle \left(\frac{\partial \langle E \rangle}{\partial r} + \langle P \rangle \frac{\partial \langle v \rangle}{\partial r} \right), \quad (16)$$

and

$$1.5 \frac{D \langle \rho W_r^2 \rangle}{Dt} = \frac{L_r \frac{\partial \langle P \rangle}{\partial r}}{\langle \rho \rangle^2 \left\langle \frac{dE}{d\rho} \right\rangle}.$$

If the pressure and entropy gradients have opposite signs, the solution is an oscillation which will decay when the dissipation is added (convective stability). If they have the same sign, the solution grows until checked by the dissipation (instability). In a star, of course, there is instability where the entropy increases toward the center.

The difference equations used in convective areas are given in the Appendix.

3. Explosions of 45, 52, and 60 M_\odot models

A. EQUATION OF STATE AND ENERGY GENERATION

The energy and pressure included the effects of radiation, ions, and electrons (including electron-positron pairs). At the comparatively low densities of these massive stars, the electronic chemical potential remains less than the electron rest mass. The integrals for the density, pressure, and energy may then be expanded in sums involving the chemical potential and the first and second Hankel functions of the second kind* with an argument of (mc^2/kT) (FOWLER and HOYLE, 1964). The chemical potential is found (in terms of the density and temperature) by the iteration of the equation for the density, a procedure that required too much time to be used each instance the potential was needed. The 'first order' potential (the value when only the first term of the sum is kept) is easily found. The difference between the potential and the first order poten-

* For temperatures less than 5.9×10^9 K, the lowest value of the argument needed for the Hankel functions is 1. For an argument greater than 5, they are given accurately by their asymptotic expansions. Between 1 and 5, the following expressions give them better than one part in 10^4 .

$K_2(z) = \exp(-z) (\pi/2z)^{1/2} (1 + 15/8z) + (2/z^2) \exp[-z(0.95851z^2 + 14.122z + 14.267)/(z^2 + 10.947z + 3.4912)],$

$K_1(z) = \exp(-z) (\pi/2z)^{1/2} + (1/z) \exp[-z(1.0103z^2 + 7.5624z + 6.1486)/(z^2 + 5.2018z + 1.3085)].$

tial was kept in tabulated form. Its value was given to sufficient accuracy by four-point interpolation in the table.

The nuclear reactions used included oxygen burning (FOWLER and HOYLE, 1964) and the α -process (FINZI and WOLF, 1966). The latter was never important. Neutrino losses included pair annihilation and the photoneutrino process. The latter (which dominates at temperatures below about $5 \times 10^8 \text{ K}$), as well as the pair annihilation under $5 \times 10^8 \text{ K}$, was calculated from its non-relativistic formula (LEVINE, 1963). For temperatures above $5 \times 10^8 \text{ K}$, pair annihilation losses were found by interpolation in the table given by CHIU (1961). The important source of opacity was electron scattering; it is somewhat greater at low densities, since the effective electron molecular weight is smaller due to the presence of pairs.

B. INITIAL MODELS

The initial models were approximately isentropic with a central temperature of $7 \times 10^8 \text{ K}$ (slightly above where neutrino losses begin to predominate over radiation losses). In the integration of the initial model, the quantity $(\partial v / \partial P) / (\partial v / \partial P)_S$ was held constant, with the values of 0.995, 0.980, and 0.995 in order of mass. The corresponding central densities were 8.44×10^3 , 7.90×10^3 , and $7.06 \times 10^3 \text{ gm/cm}^3$. The initial composition was oxygen throughout the star.

The boundary of the 'unstable area' in the temperature-density plane nearly runs along a line of constant entropy on the side where it is approached by material near the center of the star (see Figure 1). The central temperature at which a star becomes dynamically unstable is, therefore, rather sensitive to its entropy near the center. In the oxygen models used, essentially no nuclear energy was released before the point of collapse; the result was that the central entropy was quite low. Models of the same mass which were more isentropic at the point of instability should become unstable at a lower temperature. It now appears that about 25% of the helium burned in massive stars remains as carbon. The carbon is burned at a central temperature of over $1 \times 10^9 \text{ K}$, and the neon formed by the carbon will burn at a rather higher temperature. There may also be various types of shell burning during this stage of evolution. These effects are not included here; however, they may have a significant effect on the structure of the star by the time it becomes unstable.

Any low molecular weight envelope should be sufficiently extended so that it has little effect on the material near the center. The masses given then properly refer to the core mass and not the total mass of the star. It may be, however, that the mass of the envelope is small. After a central temperature of something like $7 \times 10^8 \text{ K}$, neutrino losses become the chief form of energy loss. Providing that some type of shell burning occurs at a later point in the evolution, the star will contract until the nuclear energy release is approximately that of the neutrino losses. Since the neutrino losses are concentrated near the center, and radiation losses are comparatively small, most of the energy released by the shell burning is retained in raising the entropy of the material beyond the shell. There should be enough energy to extend a convection zone over most of the exterior mass. Once the convection reaches the envelope, the

hydrogen (or helium) will be swept down into the interior and converted into high molecular weight material.

From the central temperature of $7 \times 10^8 \text{ K}$, the models took roughly 100 years to reach the point of instability. Over this period, neutrino losses increased by more than a factor of 10^4 . Figure 2 gives the temperature and density distribution of each

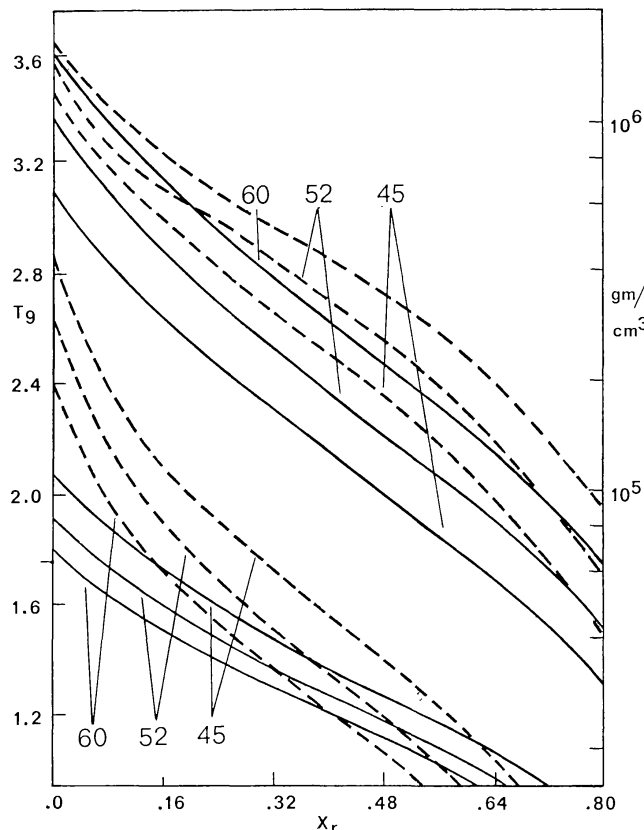


Fig. 2. The temperature (10^9 K) in solid lines and the density (gm/cm^3) in broken lines of the three models as a function of the mass fraction, X_r , at the point of instability and at the reversal of collapse.

star at the time it began to collapse. In each case it then took somewhat more than 500 sec to reach a total kinetic energy of 2×10^{48} ergs. In the description of each explosion, this was chosen as the zero point of the time.

C. COLLAPSE AND EXPLOSION

Each collapse (after reaching a kinetic energy of 2×10^{48} ergs) took around 100 sec: 76 sec (for $45 M_\odot$), 125 sec (for $52 M_\odot$), and 148 sec (for $60 M_\odot$). The peak rate of energy release by oxygen burning (reached shortly before the halt of the collapse) rose to somewhat more than 100 times the rate of the neutrino losses. Oxygen depletion was the chief reason why it did not rise higher; the mass fraction of oxygen at the center at the time of reversal of collapse was, in order of mass of the star, 0.1310, 0.0142, and 0.0026. Because the energy release was largely limited by deple-

tion, the total amount of oxygen consumed was not very sensitive to the reaction rate. With the possible exception of the $45 M_{\odot}$ model, it was estimated that a change in the reaction rate by a factor of 100 would not have altered the amount of oxygen burned by more than a factor of 2. In each case more than 80% of the energy release occurred before the reversal of collapse. The total oxygen consumed was $3.3 M_{\odot}$ ($45 M_{\odot}$), $7.3 M_{\odot}$ ($52 M_{\odot}$), and $15 M_{\odot}$ ($60 M_{\odot}$). The energy release is about 1.0×10^{51} ergs per M_{\odot} . Figures 3, 4, and 5 give the rate of energy release, as well as neutrino losses, as a function of time. They also give the total energy, turbulent energy (produced by convection), and kinetic energy.

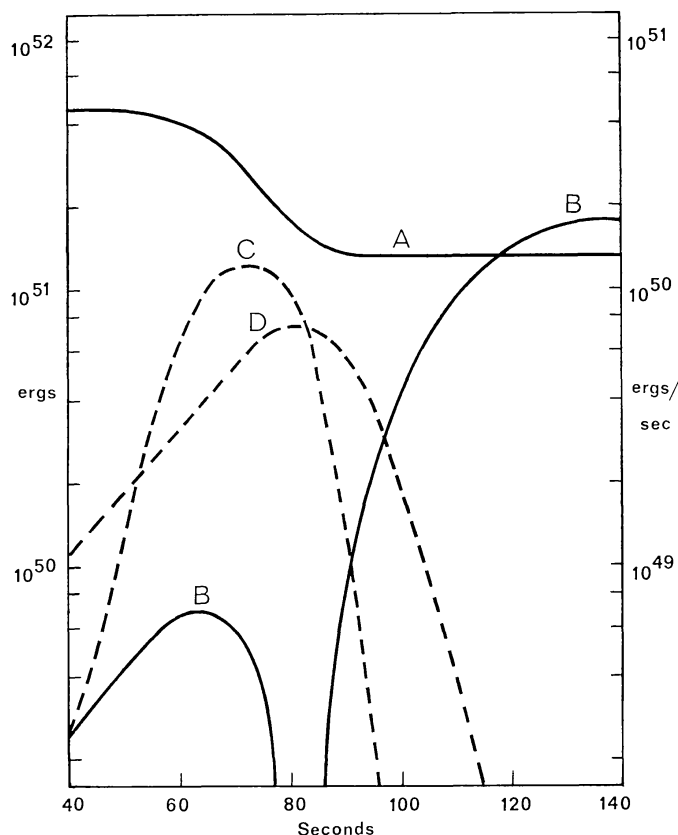


Fig. 3. The absolute value of the total energy (A), the kinetic energy (B), the rate of nuclear energy release (C), and the neutrino losses ($\times 100$) (D) of the $45 M_{\odot}$ model as a function of time.

Each model first became convectively unstable at a mass fraction, X_r , of about 0.08. For the $45 M_{\odot}$ model, this occurred at 82 sec (6 sec after the reversal of collapse). The convective zone eventually extended to $X_r=0.12$. In the $52 M_{\odot}$ case, convection started at 116 sec, and at the reversal of collapse it has spread to $X_r=0.28$. At its maximum extent, it reached $X_r=0.56$. As the entropy gradient in the outer part of the star was small, a slightly larger release of energy would probably have extended the convection to the surface. In the $60 M_{\odot}$ model, convection started at 137 sec, reaching $X_r=0.56$ at 148 sec, $X_r=0.82$ at 156 sec, and the surface by 162 sec. The

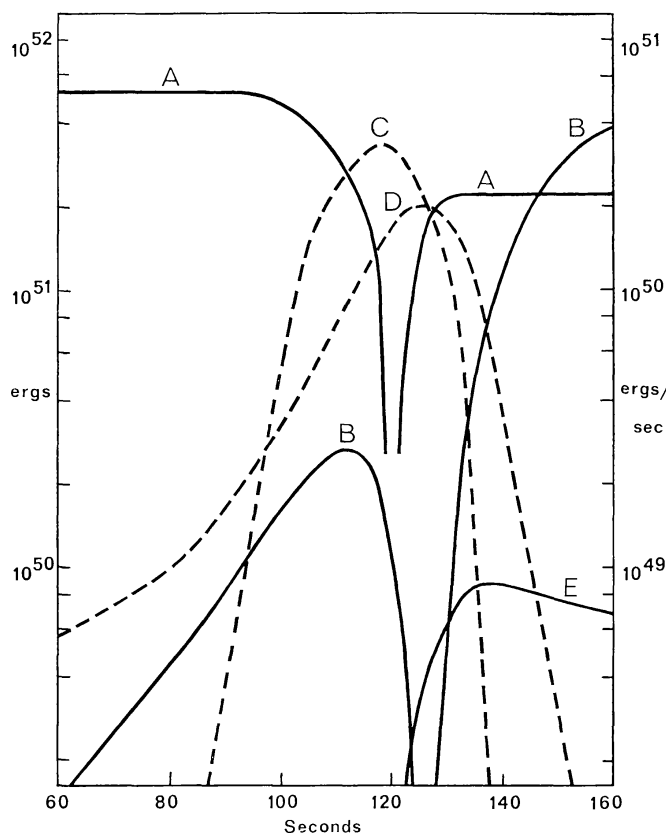


Fig. 4. The quantities of Figure 3, as well as the turbulent energy (E), for the $52 M_{\odot}$ model.

last two figures are not very meaningful. There was no energy generation in the outer part of the star, and the front of the convection zone moved considerably faster than the speed of the turbulence; this would not seem to be physically possible. The convective equations represent a type of diffusion, and so are not very satisfactory in describing the advance of a quickly moving convection front. With the equations used, the convection crossed a mass zone in the time it took the zone to absorb enough energy to raise its entropy above that of the next zone; this occurs rapidly for nearly isentropic material.

The large entropy gradient near the center produced by the high temperature dependence of the neutrino losses was apparently the cause of the convection starting away from the center. Ordinarily this would be more than offset by the even higher temperature dependence of the nuclear reaction rate; however, in this case, the collapse quickly pushed the material to high temperatures where the temperature dependence of the oxygen burning is lower. This and oxygen depletion, which also reduced the differential of the energy release throughout the star, caused the convection to start away from the center where the entropy gradient was lower.

The convection probably did not have much effect on the explosions. The maximum turbulent energy density was less than 1% of the internal energy density. (The largest speed of turbulence was about 1000 km/sec.) The evolution was too fast by

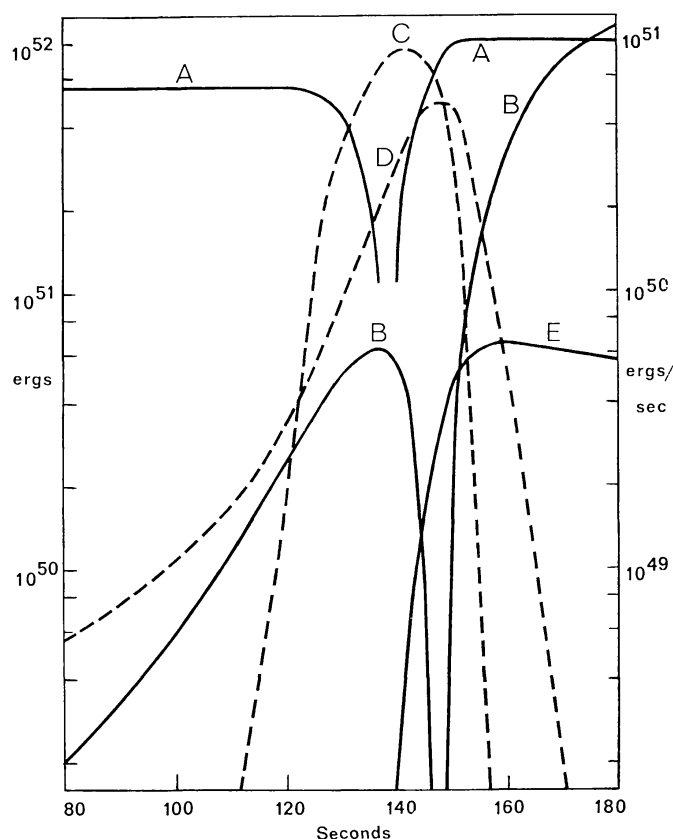


Fig. 5. The quantities of Figure 4 for the $60 M_{\odot}$ model.

about a factor of 10 to produce much mixing. The convective mixing increased the total amount of material burned by only a few percent. (The effect may have been more important if the convection had started at the center.) The 'implicit' equations used for the calculation of the convection (see Appendix) will, if anything, overestimate the rate of growth of the convection. In a calculation on a $40 M_{\odot}$ star, BARKAT *et al.* (1967) estimated the effects of convection by first assuming no mixing and then complete mixing. In the latter case, twice as much oxygen was burned. In the $60 M_{\odot}$ star, the convection carried about 7×10^{49} ergs to the surface.

In each case, as the collapse reversed, and the star began to expand, no shock wave was observed to develop, except possibly in the outer few percent of the mass. The rate of energy release was quite low compared to that necessary to develop a shock in the interior. The power to do this, as estimated by ONO and SAKASHITA (1962), is $3 \times 10^{46} \times (M/R)^{2.5}$ ergs/sec (mass and radius in terms of those of the sun). This is about 1000 times the actual rate.

After the collapse was halted, the basic feature was the increase in kinetic energy. The $45 M_{\odot}$ model was the only one in which the total energy remained negative; this meant that the whole star would not be disrupted, but it did not prevent some of the material from being ejected. At 145 sec, the kinetic energy reached its maximum of 1.81×10^{51} ergs, the surface velocity being 4337 km/sec. At 189 sec, the surface ve-

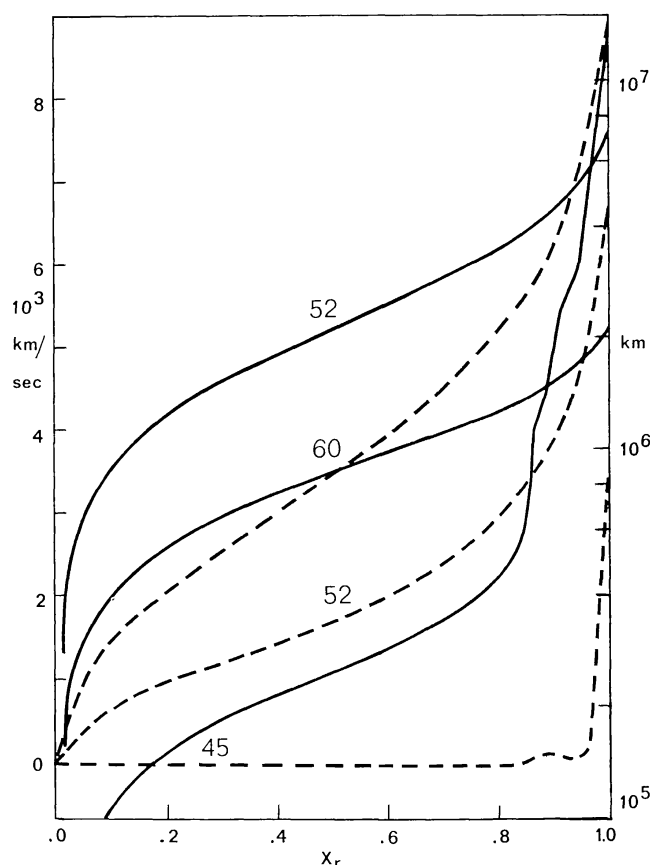


Fig. 6. The radius (solid lines) and velocity distribution (broken lines) at the time at which calculations for each model were terminated.

locity reached a maximum of 4652 km/sec (about $\frac{1}{3}$ the escape velocity at maximum contraction). At 940 sec, about the inner 90% of the star began to collapse again (the central density then being 300 gm/cm³). This produced an oscillation with a period of 1300–1400 sec; slightly more than two periods were followed. During the first oscillation, the central density increased by a factor of 30, and then expanded by a factor of 10. During the second oscillation, the corresponding factors were 5 and 3. At least initially the oscillation was being rapidly damped out. The chief cause of the damping was probably the interaction with the ejected material, the oscillation producing shock waves which reinforced the motion of the outer part of the star. The evolution was followed to about 4000 sec. Conditions at this time indicated a final velocity at the front of the ejected material of around 3400 km/sec. From 1 to 2 M_{\odot} were ejected (i.e., had a velocity greater than the velocity of escape).

The kinetic energy of the 52 M_{\odot} model reached a maximum of 4.88×10^{51} ergs at 191 sec, with a surface velocity of 6400 km/sec. The latter reached its maximum of 6774 km/sec at 310 sec. After this the velocity decreased only slightly. The evolution was followed to 1257 sec, where it was 6622 km/sec. By subtracting the gravitational energy from the kinetic energy, the final velocity was estimated to be at least 6500 km/sec. The point in the star at which the velocity equalled the velocity of escape

indicated at least $20 M_{\odot}$ would be ejected. Since the total energy of the star was positive, it may be that essentially all the mass would be found to be ejected if the evolution were followed long enough.

The kinetic energy of the $60 M_{\odot}$ model reached its maximum of 1.09×10^{52} ergs at 224 sec; the surface velocity was 8741 km/sec. This reached 8948 km/sec at 345 sec. The evolution was followed to 390 sec. By the same methods as before, the final velocity was found to be greater than 8500 km/sec, and at least $40 M_{\odot}$ were ejected.

D. SUMMARY

The velocities given in Table I (the averaged velocity of about the outer 1% of the mass) would be modified somewhat if an envelope had been added to the calculations. They are comparable to those observed in type II supernovae (5000–10000 km/sec); however, there is still a question of how and where in the star the observed (Doppler-shifted) light originates. The masses of the supernovae do not seem to be wellknown. Estimates of from 1 to $10 M_{\odot}$ have been given. One estimate of $60 M_{\odot}$ was made by SHKLOVSKII (1960).

TABLE I
Results

Mass	Mass Ejected	Mass of Oxygen Burned	Velocity of Expansion
45	1–2	3.3	3400
52	20–52	7.3	6500
60	40–60	15.	8500

Appendix: Difference Equations

The equations of momentum and energy conservation under spherical symmetry are:

$$\frac{\partial U}{\partial t} = -4\pi R^2 \frac{\partial P}{\partial M} - \frac{GM}{R^2}, \quad (17)$$

and

$$\frac{\partial E}{\partial t} + P \frac{\partial v}{\partial t} = \varepsilon - \frac{\partial F}{\partial M}. \quad (18)$$

The independent variables are the time t , and M , the total interior mass; F is the total energy flux across a spherical surface, ε is the specific rate of energy generation, and U is the radial velocity.

A. FINITE DIFFERENCE APPROXIMATIONS

In the numerical calculation of the evolution, the star is divided into N mass zones. The boundaries of the zones are denoted by integers, and the midpoints by half-integers. The specific volume, temperature, composition, and quantities depending on them, such as the pressure and opacity, are defined at the midpoints. The velocity,

radius, and energy flux are defined at the boundaries. The size of the time step is $DT (= t^{n+1} - t^n)$. The mass of the zone centered at $I - \frac{1}{2}$ is $\Delta M(I - \frac{1}{2})$; the mass interior to I is $M(I)$. The average value of a quantity over the time step is denoted by enclosing it in $\langle \rangle$. Equations (17) and (18) are then approximated by

$$\frac{D[U(I)]}{DT} = -4\pi \langle R(I)^2 \rangle \frac{\Delta \langle P(I) \rangle}{\Delta M(I)} - GM(I) \left\langle \frac{1}{R(I)^2} \right\rangle, \quad (19)$$

and

$$D[E(I - \frac{1}{2})] + \langle P(I - \frac{1}{2}) \rangle_E D[v(I - \frac{1}{2})] = DT \left[\langle \varepsilon(I - \frac{1}{2}) \rangle - \frac{\Delta \langle F(I - \frac{1}{2}) \rangle}{\Delta M(I - \frac{1}{2})} \right], \quad (20)$$

where

$$\Delta M(I) = 0.5 [\Delta M(I - \frac{1}{2}) + \Delta M(I + \frac{1}{2})].$$

D indicates a time difference, and Δ a radial difference, e.g.,

$$\begin{aligned} D[U(I)] &= U(I)^{n+1} - U(I)^n, \\ \Delta \langle P(I) \rangle &= \langle P(I + \frac{1}{2}) \rangle - \langle P(I - \frac{1}{2}) \rangle, \end{aligned}$$

and

$$\Delta \langle F(I - \frac{1}{2}) \rangle = \langle F(I) \rangle - \langle F(I - 1) \rangle.$$

The radius is given by

$$R(I)^{n+1} = R(I)^n + DT \langle U(I) \rangle.$$

The specific volume at $I - \frac{1}{2}$ is defined as the total volume of the zone divided by its mass. The usual method of averaging is to take a weighted sum of the early time value (at t^n) and of the late time value (at t^{n+1}). The averaged pressure also includes the artificial viscosity used to handle shock waves (RICHTMYER, 1957).

As the basic interest was in processes in the interior, conditions at the surface were not treated precisely. The surface is defined by zero pressure. Equation (19) may be used at the surface by defining

$$\langle P(N + \frac{1}{2}) \rangle = 0, \quad \Delta M(N) = 0.5 \Delta M(N - \frac{1}{2}).$$

The way in which the radii are averaged is determined by energy conservation. The total energy is defined as

$$E_T = \sum_{I=1}^N \left[\Delta M(I - \frac{1}{2}) E(I - \frac{1}{2}) + 0.5 \Delta M(I) U(I)^2 - \frac{GM(I) \Delta M(I)}{R(I)} \right]. \quad (21)$$

Providing the average velocity has a time-centered definition (i.e., an equal weighting is given to late and early time values), and the average pressure used in Equation (19) is the same as that used in Equation (20), the total energy is conserved if

$$\langle R(I)^2 \rangle = \frac{1}{3} [R(I)^{n+1} R(I)^{n+1} + R(I)^{n+1} R(I)^n + R(I)^n R(I)^n]$$

and

$$\left\langle \frac{1}{R(I)^2} \right\rangle = \frac{1}{R(I)^{n+1} R(I)^n}.$$

Where the average velocity is given by

$$\langle U(I) \rangle = \alpha U(I)^{n+1} + (1 - \alpha) U(I)^n,$$

the energy is increased too much by

$$\sum_{I=1}^N (0.5 - \alpha) \Delta M(I) D[U(I)]^2.$$

This suggests that the best value of α is 0.5 or slightly greater.

Except for large time steps where stability considerations become more important, time-centered equations should usually be more accurate. These were found to be marginally stable, i.e., perturbations and irregularities persisted over a number of time steps with about the same magnitude. (The size of the time steps were determined by the rate of change of conditions only, and no attempt was made to keep them below, e.g., the Courant limit.) When the late time weightings were increased slightly, e.g., to 0.51, the equations were stabilized.

For sufficiently slow evolution, it was found better to use the 'hydrostatic' equation. All 'averaged' quantities in the acceleration Equation (19) were given their late time values. The acceleration is then equated to the force at t^{n+1} , and as the acceleration is small, the force is effectively put equal to zero. It is preferable to have a time-centered value of the average pressure in the energy Equation (20). The energy, as given in Equation (21), is then no longer formally conserved. However, where the maximum density changes over a time step were kept sufficiently small (less than 5–10%), the energy was usually conserved within an acceptable accuracy.

The equations are solved by linearizing them and solving the linearized forms. This process is iterated until the equations are satisfied. As the linearization did not always work, supplementary procedures had to be added. They consist basically in limiting the amount the variables can change during each iteration.

With nuclear reactions present, we also need an equation for the change of each isotope over the time step. The change in a mass fraction due to a given reaction is proportional to the average energy generation of that reaction. It is necessary to define this so that each mass fraction remains between 0 and 1. This may be done by averaging separately its composition dependence and its dependence on temperature and density. If a reaction's dependence on a given mass fraction is X^v , then the average value at $I - \frac{1}{2}$ is given by

$$\langle X(I - \frac{1}{2})^v \rangle = X(I - \frac{1}{2})^{n+1} [X(I - \frac{1}{2})^n]^{v-1}.$$

At the densities at which investigations were carried out, virtually all neutrinos escape directly from the star. Neutrino losses are then treated as a negative rate of energy generation.

B. CONVECTIVE DIFFERENCE EQUATIONS

In convective areas, the difference equations are based on Equations (8), (12), (14), and (15), which are given in Section 2. The averaged speed of the convective turbu-

lence ($\langle |W_r| \rangle$) and of the total convective energy flux ($4\pi r^2 L_r$) are defined at the boundary of each mass zone as $W(I)$ and $L(I)$. Often the relaxation time for the convection is much less than the characteristic time of evolution of the star. The convection is then approximately in equilibrium, and as the time step is usually taken proportional to the evolutionary time-scale, the (dynamical) difference equations for the convection must reduce to the equilibrium case for these large time steps. This is done by giving all quantities on the right-hand side of the difference forms of Equations (12) and (14) their values at t^{n+1} (as was done for the acceleration equation under hydrostatic conditions).

The pressure-like effect of the Reynolds stresses is defined at $I - \frac{1}{2}$ as $S(I - \frac{1}{2})$. This was usually given the averaged value

$$\langle S(I - \frac{1}{2}) \rangle = 0.5 [W(I - 1)^2 + W(I)^2] / v(I - \frac{1}{2}).$$

(Unless otherwise indicated, all quantities not enclosed by $\langle \rangle$ represent their values at t^{n+1} .) For simplicity, the ratio of the enthalpy to the energy was given a constant value γ_1 . Then the momentum and energy equations become

$$\frac{D[U(I)]}{DT} = - \frac{4\pi \langle R(I)^2 \rangle}{M(I)} [\Delta \langle P(I) \rangle + \Delta \langle S(I) \rangle] - GM(I) \left\langle \frac{1}{R(I)^2} \right\rangle, \quad (22)$$

and

$$\begin{aligned} D[E(I - \frac{1}{2})] + [\langle P(I - \frac{1}{2}) \rangle_E + \langle S(I - \frac{1}{2}) \rangle] D[v(I - \frac{1}{2})] + 0.75 D[W(I)^2] \\ + 0.75 D[W(I - 1)^2] = DT \left\{ \langle \varepsilon(I - \frac{1}{2}) \rangle \right. \\ \left. - \frac{[\gamma_1 \Delta \langle L(I - \frac{1}{2}) \rangle + \Delta \langle F(I - \frac{1}{2}) \rangle]}{\Delta M(I - \frac{1}{2})} \right\}. \quad (23) \end{aligned}$$

F is now the non-convective energy flux. Equation (15) instead of (5) is used as the basis of the energy Equation (23). While the change in the turbulent energy is often small, the rate at which it is being produced and dissipated may be quite large (and nearly cancel). By using Equation (15), two large non-linear terms are replaced by two smaller, more linear quantities, which is to be preferred in numerical work. $U(I)$ now indicates the average radial velocity.

$Y(I)$ is the mean of $(d\varepsilon/dE)$ at $I - \frac{1}{2}$ and $I + \frac{1}{2}$; the convective equations are then

$$\begin{aligned} \frac{D[L(I)]}{DT} = \frac{-32\pi^2 R(I)^4 W(I)^2}{\{\Delta M(I) [v(I - \frac{1}{2})^2 + v(I + \frac{1}{2})^2]\}} \{0.5 [P(I - \frac{1}{2}) + P(I + \frac{1}{2})] \Delta [v(I)] \\ + \Delta [E(I)]\} + L(I) \left[Y(I) - \frac{4\pi R(I)^2 [U(I + 1) - U(I - 1)]}{\{\Delta M(I) [v(I - \frac{1}{2}) + v(I + \frac{1}{2})]\}} - \frac{W(I)}{l(I)} \right], \quad (24) \end{aligned}$$

and

$$\begin{aligned} \frac{D[1.5 W(I)^2]}{DT} = \frac{-L(I) [\gamma_2 - 1] \Delta [P(I)]}{\{\Delta M(I) 0.5 [P(I + \frac{1}{2}) + P(I - \frac{1}{2})]\}} - \frac{W(I)^3}{l(I)} \\ - 0.5 W(I)^2 \left\{ \frac{D[v(I - \frac{1}{2})]}{v(I - \frac{1}{2})} + \frac{D[v(I + \frac{1}{2})]}{v(I + \frac{1}{2})} \right\}, \quad (25) \end{aligned}$$

where $(\gamma_2 - 1) = -P/(dE/d\rho \rho^2)$ and is held constant at some mean value. The term $l(I)$ is defined within a coefficient as the minimum of the pressure scale height, the radius, and the length of the convection zone. Radiative dissipation was not important for the conditions under consideration, so this was neglected.

Instability is considered to exist at I when the term

$$-0.5 [P(I - \frac{1}{2}) + P(I + \frac{1}{2}) \Delta[v(I)] - \Delta[E(I)]]$$

becomes positive. This is tested for at the beginning of each time step and, optionally, at several times during the iteration process as the equations are being solved. The convection equations are then applied until the turbulence has died out, which will be a number of time steps after the boundary has become stable again. When the sum

$$\sum_{I=1}^N 1.5 \Delta M(I) W(I)^2$$

is added to the definition of the total energy, it is conserved to the same extent as before.

When convective diffusion is added, the rate of change of an isotope is

$$\frac{DX}{Dt} = XP - \frac{\partial}{\partial r} [r^2 \langle \rho W_r X \rangle] / (\langle \rho \rangle r^2), \quad (26)$$

where XP is the rate it is being produced by reactions. This is approximated by

$$\frac{D[X(I - \frac{1}{2})]}{DT} = \langle XP(I - \frac{1}{2}) \rangle + \frac{2\pi}{[\Delta M(I - \frac{1}{2}) v(I - \frac{1}{2})]} \{R(I)^2 W(I) \Delta[X(I)] - R(I - 1)^2 W(I - 1) \Delta[X(I - 1)]\}. \quad (27)$$

Acknowledgments

I would like to express my thanks to Professor Robert F. Christy for his advice and suggestions. I am grateful to the National Aeronautics and Space Administration for financial support, including that under Grant NsG-426.

References

- ARNETT, D.: 1967, *Can. J. Phys.* **45**, 1621.
 BARKAT, Z., RAKAVY, G., and SACK, N.: 1967, *Phys. Rev. Letters* **18**, 379.
 BATCHELOR, G. K.: 1953, *The Theory of Homogeneous Turbulence*, The University Press, Cambridge, pp. 103–116.
 CHIU, H. Y.: 1961, *Phys. Rev.* **123**, 1040.
 COLGATE, S. A. and WHITE, R. H.: 1966, *Astrophys. J.* **143**, 626.
 COWLING, T. G.: 1936, *Monthly Notices Roy. Astron. Soc.* **96**, 42.
 FINZI, A. and WOLF, R. A.: 1966, submitted for publication.
 FOWLER, W. A. and HOYLE, F.: 1964, *Astrophys. J. Suppl.* **91**, Vol. IX, 201.
 LEVINE, M. J.: 1963, Ph.D. thesis, California Institute of Technology (unpublished).
 ONO, Y. and SAKASHITA, S.: 1962, *J. Phys. Soc. Japan* **17**, Suppl. A-III, 153.
 RAKAVY, G. and SHAVIV, G.: 1966, submitted for publication.
 RICHTMYER, R. D.: 1957, *Difference Methods for Initial-Value Problems*, Interscience Publishers, Inc., New York, pp. 208–215.
 SHKLOVSKII, I. S.: 1960, *Sov. Astron.* **4**, 355.